NANO LETTERS

pubs.acs.org/NanoLett Letter

Unveiling Mechanical Activation: GAIN Domain Unfolding and Dissociation in Adhesion GPCRs

Chaoyu Fu,[#] Wenmao Huang,[#] Qingnan Tang,[#] Minghui Niu, Shiwen Guo, Tobias Langenhan, Gaojie Song,[*] and Jie Yan[*]

Cite This: https://doi.org/10.1021/acs.nanolett.3c01163 Read Online

ACCESS | Metrics & More | Article Recommendations | Supporting Information

ABSTRACT: Adhesion G protein-coupled receptors (aGPCRs) have extracellular regions (ECRs) containing GPCR autoproteolysis-inducing (GAIN) domains. The GAIN domain enables the ECR to self-cleave into N- and C-terminal fragments. However, the impact of force on the GAIN domain's conformation, critical for mechanosensitive aGPCR activation, remains unclear. Our study investigated the mechanical stability of GAIN domains in three aGPCRs (B, G, and L subfamilies) at a loading rate of 1 pN/s. We discovered that forces of a few piconewtons can destabilize the GAIN domains. In autocleaved aGPCRs ADGRG1/GPR56 and ADGRL1/LPHN1, these forces cause the GAIN domain detachment from the membrane-proximal Stachel sequence, preceded by partial unfolding. In non-cleavable aGPCR ADGRB3/BAI3 and cleavage-deficient mutant ADGRG1/GPR56-T383G, complex mechanical unfolding of the GAIN domain occurs. Additionally, GAIN domain detachment happens during cell migration. Our findings support the mechanical activation hypothesis of aGPCRs, emphasizing the sensitivity of the GAIN domain structure and detachment to physiological force ranges.

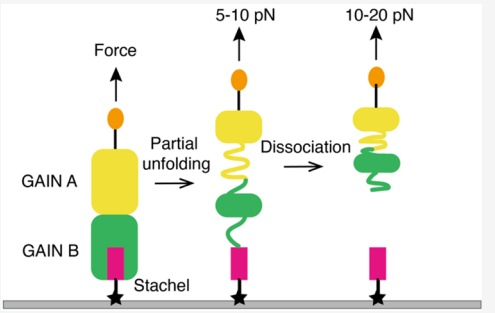

KEYWORDS: *adhesion GPCR, GAIN domain unfolding, GAIN domain dissociation, GPR56, LPHN1, BAI3*

G protein-coupled receptors (GPCRs) are transmembrane receptors, and the majority of them are activated by extracellular ligands. The binding of these ligands induces a conformational change in the receptor's extracellular region or seven transmembrane (7TM) domains. This crucial process facilitates cellular signaling and has undergone thorough investigation.[1]

GPCRs are classified into five major families.[2−5] The adhesion GPCRs (aGPCRs) are the second largest family, with 33 mammalian homologues.[2] Most aGPCRs have a large extracellular N-terminal region (ECR) that enables adhesive interactions with the extracellular matrix (ECM) or neighboring cell membrane proteins.[6−9] Thirty-two of the 33 mammalian aGPCRs feature a conserved GPCR autoproteolysis-inducing (GAIN) domain with a GPCR proteolysis site (GPS) embedded within it.[8,10,11] The GAIN domain contains a tethered agonist element (Stachel), essential for aGPCR activation.[12,13]

In some aGPCRs, the GAIN domain is capable of undergoing autoproteolysis, resulting in the formation of two noncovalently associated fragments: the N-terminal fragment (NTF) and the rest of the receptor, which is referred to as the C-terminal fragment (CTF).[11,14−17] The CTF consists of the Stachel that is connected to the first transmembrane helix of the 7TM domain.[8,12,13] However, self-cleavage is not a general feature of aGPCRs as the GAIN domains of a few aGPCRs are incapable of self-proteolysis (see reviews in refs 9 and 18).

aGPCRs are crucial in various biological processes such as neuronal development, immune cell function, and cancer progression.[19−23] However, their activation mechanisms are incompletely understood. Activation requires an endogenous Stachel within the GAIN domain.[12,13] Two models explain Stachel exposure: the dissociation (one-and-done) model, involving NTF/CTF heterodimer disruption,[12,24−26] and the nondissociation (tunable) model, with partial allosteric movements in intact NTF/CTF aGPCR heterodimers.[10,13,17,27,28] Recent structural studies support both scenarios,[29−35] and the existence of self-cleavable and noncleavable aGPCRs highlights the feasibility of both models, complicating pharmacological advances.

Several self-cleavable[25,36−40] and noncleavable[41] aGPCRs show sensitivity to mechanical stimuli applied to their NTFs, indicating mechanical activation as an adequate mode of activation. However, the exact mechanism of this mechanical activation process remains unknown. A mechanical activation model has been proposed, where force-induced NTF/CTF dissociation exposes the Stachel to activate aGPCRs.[42−45]

Received: March 29, 2023
Revised: August 4, 2023

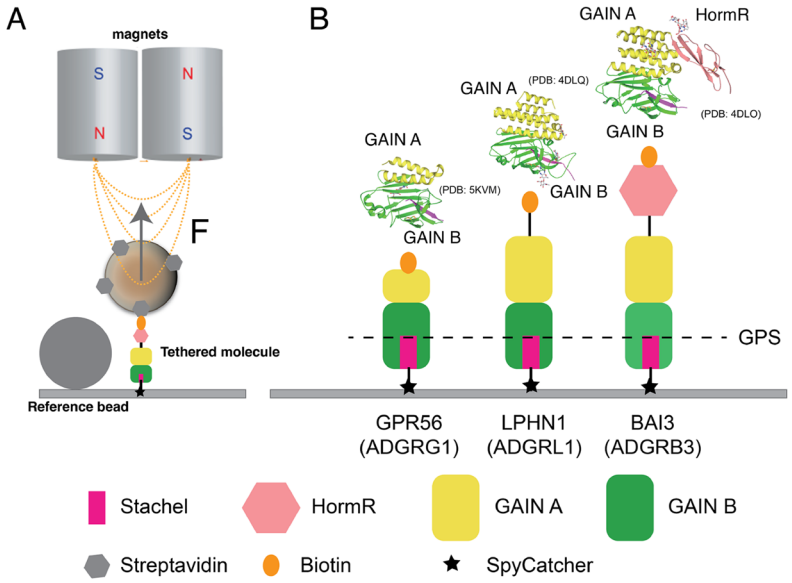

Figure 1. System setup and tethered configuration of GPR56, LPHN1, and BAI3. (A) An aGPCR's GAIN domain tethered between a 2.8-μm-diameter superparamagenetic bead is subjected to an external force exerted by a pair of permanent magnets. (B) The GAIN domains of GPR56, LPHN1, and BAI3 are depicted in the illustration. The GPS are located within the GAIN B subdomains.

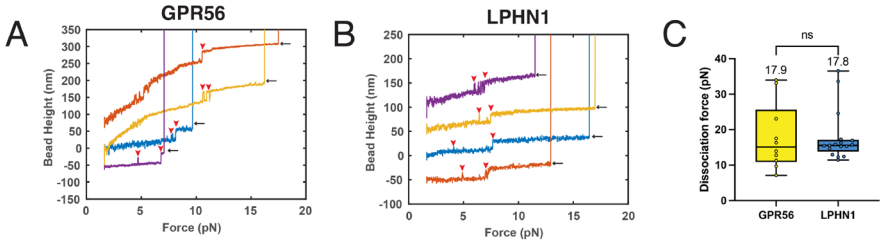

Figure 2. NTF/CTF dissociation of GAIN domains of GPR56 and LPHN1. (A) Representative force−bead height curves of four tethers for GPR56's GAIN domain during force loading until NTF/CTF dissociation. Black arrow: NTF-CTF dissociation event; red arrowhead: GAIN domain unfolding event. (B) Representative force−bead height curves of four independent tethers for LPHN1's GAIN domain during force loading until NTF/CTF dissociation. Black arrow: NTF-CTF dissociation event; red arrowhead: GAIN domain unfolding event. (C) Box plots of forces where NTF/CTF dissociation events were observed, which provides information on the medians and IQRs. The means are indicated. A fixed loading rate of 1.0 ± 0.1 pN/s was applied.

Similarly, mechanical activation can also explain nondissociative aGPCR activation, where forces applied to NTFs may allosterically change the GAIN domains conformation and transiently expose the Stachel.[17,41]

It remains unclear whether the typical physiological range of forces, which vary from a few piconewtons (pN) to tens of pN,[46,47] can induce NTF/CTF dissociation or significant conformational changes in the GAIN domains. To bridge this knowledge gap between mechanical activation models of aGPCRs and their physiological functions, we investigated the force-response of the GAIN domains of three representative aGPCRs, including ADGRG1/GPR56 and ADGRL1/LPHN1, which both possess cleavability but different GAIN domain organizations, as well as ADGRB3/BAI3, which has a noncleavable GAIN domain. We applied forces to individual GAIN domains and recorded their force-dependent dissociation/conformational changes using an in-house constructed magnetic-tweezers setup.[48,49] We also investigated the effect of cell migration on the dissociation of the NTF/CTF of GPR56 by using a surface-bound artificial ligand that forms a covalent bond with the N-terminus of GPR56.

Our results reveal that (1) the subdomains in the GAIN domain undergo structural unfolding within forces of a few pN; (2) for aGPCRs with cleavable GAIN domain, NTF/CTF dissociation occurs following domain partial unfolding; and (3) the NTF/CTF dissociation can occur during cell migration when the aGPCR-extracellular matrix (ECM) linkage is sufficiently stable. Our results provide a physical basis that sheds light on the two mechanical activation models and how cell migration could play a role in the activation of the receptors.

DISSOCIATION OF GPR56 AND LPHN1 DURING FORCE LOADING

Figure 1 shows illustrations of the experimental design and protein constructs used in this study. The cleavable GPR56 construct contains a cleavable GAIN domain, with two α-helices in its GAIN A subdomain.[50] The cleavable LPHN1 construct contains a GAIN domain consisting of a six-helix GAIN A subdomain and a GAIN B subdomain with similar corresponding structures to those in the noncleavable BAI3.[11] BAI3 construct includes an additional HormR domain at the N-terminus.

https://doi.org/10.1021/acs.nanolett.3c01163
Nano Lett. XXXX, XXX, XXX−XXX

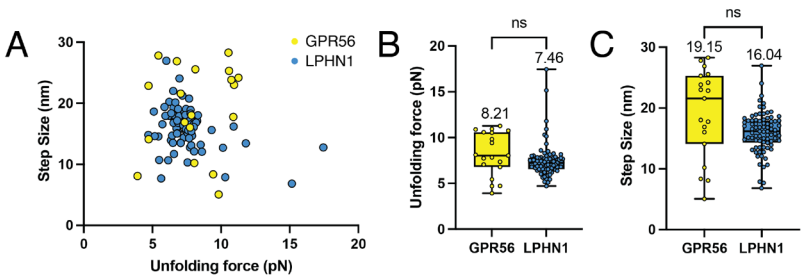

Figure 3. Force-induced unfolding of GAIN domains of GRP56 and LPHN1. (A) Two-dimensional scatter plot depicting the force-step size data for the unfolding steps preceding the dissociation of NTF/CTF. (B and C) Box plots of forces (B) and step sizes (C) where unfolding events were observed, which provides information on the medians and IQRs. The means are indicated. A fixed loading rate of 1.0 ± 0.1 pN/s was applied.

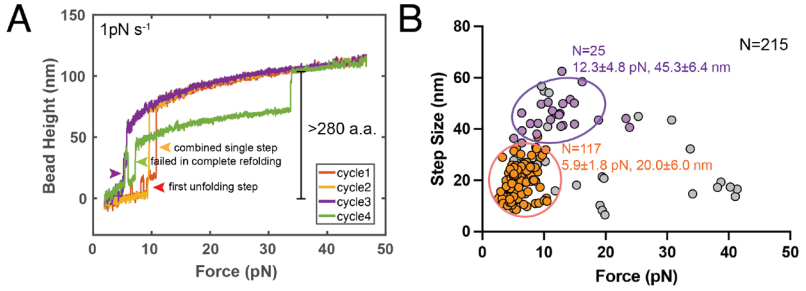

Figure 4. Force-induced unfolding of the GAIN domain of BAI3. (A) The panel shows representative bead height-force curves obtained from successive force loading processes at a loading rate of 1.0 ± 0.1 pN/s. Multiple steps of unfolding events were observed in each force loading process. Two unfolding steps (red and purple arrows), which sometimes combined into a single step of unfolding (orange arrow), occurred at forces from 5 to 10 pN. In some force-loading cycles, the unfolded BAI3 failed in complete refolding during holding the tether for 30 s at 1 pN before the next force-loading process, which is indicated by a greater bead height (green arrow). (B) The panel shows a 2D scatter plot of the force−step size data for the unfolding events. Data within the orange circles represent the first unfolding events, which are similar to those observed for the GAIN domains of GPR56 and LPHN1 prior to NTF/CTF dissociation. Data in gray indicate the second unfolding event, while data within the purple circle correspond to the combination of two unfolding steps into a single step.

Each construct has a biotinylated AVI tag at the N-terminus and a SpyTag at the C-terminus. The C-terminus is immobilized to a SpyCatcher-coated coverslip surface,[51] while the N-terminus is linked to a 2.8-μm-diameter superparamagnetic microbead (Figure 1). Forces are applied to individual protein tethers using a magnetic tweezers setup,[48,49] by attaching one end of the microbead to a pair of permanent magnets placed above the chamber. The magnitude of the force is controlled by adjusting the magnet−bead distance, and the change in bead height from the coverslip surface is recorded at nanometer resolution with a sampling rate of 200 Hz. Details of the single-molecule manipulation using magnetic tweezers are available in our previous publications[48,49] and are also briefly shown in Supplementary Text S1.

We first examined the mechanical response of the GPR56's GAIN domain to an increasing force at a loading rate of 1.0 ± 0.1 pN/s. Figure 2A displays representative bead height changes from four independent tethers. The curves are shifted along the *y*-axis for better visualization. We note that while the change in bead height is a result of both bead rotation and extension change of the molecule during force change, the bead height change during a stepwise change is equivalent to the molecular extension change.[49]

At this loading rate, the force−bead height data reveal structural transitions at forces between 5 and 10 pN, indicated by stepwise height changes (Figure 2A). The tethers were broken when the forces were further increased. The same type of experiments conducted for LPHN1 revealed similar mechanical responses over a similar force range (Figure 2B).

Figure 2C summarizes the NTF/CTF dissociation forces obtained for more than 10 tethers for each construct. The forces were found distributed with interquartile range (IQR) from 10 to 20 pN for the GPR56's GAIN domain and 14−17 pN for LPHN1's GAIN domain. These results suggest that NTF/CTF dissociation for both GPR56 and LPHN1 occurs within a comparable force range of 10−20 pN at our loading rate.

FORCE-DEPENDENT GAIN DOMAIN STRUCTURAL CHANGES OF GPR56 AND LPHN1

As shown in Figure 2, extensive structural changes of the GAIN of GPR56 and LPHN1 occurred at forces before NTF/CTF dissociation, indicated by stepwise extension increases (unfolding) during force loading. These force-dependent unfolding events (more than 50) from more than 10 tethers are represented in force-step size graphs (Figure 3A), box plots of the unfolding forces (Figure 3B), and unfolding step sizes (Figure 3C).

The data show that the majority of unfolding forces for both GAIN domains occur over a force range from 5 to 10 pN. The step sizes mainly range from 10 to 30 nm. Notably, the domain unfolding forces are smaller than the NTF/CTF dissociation forces, as can be seen by the comparison between Figures 2C and 3B. By analyzing the unfolding step sizes and considering the sizes of the GAIN A and GAIN B subdomains of GPR56, the unfolding signals preceding the NTF/CTF dissociation involve partial unfolding of the GAIN B subdomain (Supplementary Text S2). The similar unfolding signals observed for LPHN1 preceding the NTF/CTF dissociation

https://doi.org/10.1021/acs.nanolett.3c01163
Nano Lett. XXXX, XXX, XXX−XXX

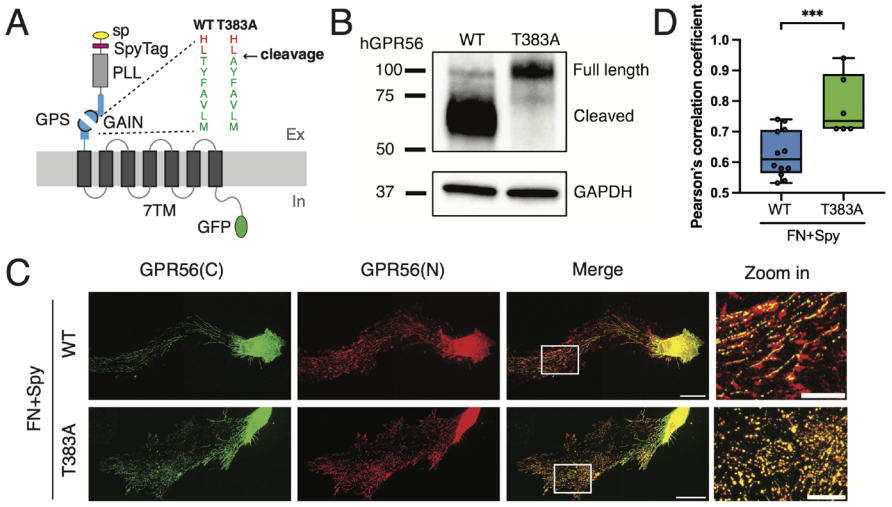

Figure 5. GPR56 NTF/CTF dissociation during cell migration. (A) Schematic of the GPR56 fusion protein used in the study. The extracellular domain of GPR56 consists of a signal peptide (sp), a SpyTag, a Pentraxin/Laminin/neurexin/sex-hormone-binding-globulin-Like (PLL), and a GAIN domain. The GAIN domain is cleaved between amino acids 382 and 383 at a conserved GPS. A noncleavable mutant of GPR56 (Spy-GPR56-T383A-GFP) was created suppressing cleavage of the GAIN domain. (B) Western blot of whole-cell lysates from HFF cells expressing either the wild-type GPR56 construct (Spy-GPR56-WT-GFP) or the noncleavable construct (Spy-GPR56-T383A-GFP). (C) HFF cells were transfected with either Spy-GPR56-WT-GFP or Spy-GPR56-T383A-GFP constructs and then spread and migrated on surfaces coated with FN +Spy. NTF-CTF dissociation was measured by loss of colocalization of the C-terminal fragment, which is visualized by GFP (green), and N-terminal fragment, which is visualized by the staining of antibody targeting NTF (red). Scale bars: 30 μm for merge, 10 μm for zoom-in. (D) Pearson's correlation coefficient between the N-terminal fragment (GPR56-N) and the C-terminal fragment (GPR56-C) of GPR56 in the conditions of c ($N > 5$).

suggest that it may also involve the partial unfolding of the GAIN B subdomain.

To investigate the relationship between force-induced GAIN domain unfolding and NTF/CTF dissociation, we introduced the T383G mutation in GPR56.[11] The mutated GAIN domain remained intact up to 50 pN (Figure S1A-B). Similar to wild-type GPR56, we also observed the partial unfolding of the GAIN B subdomain in GPR56-T383G, characterized by a circled cluster of data with an unfolding force ranging between 5 and 10 pN and an unfolding step size between 10 and 30 nm (Figure S1B–D). Notably, higher forces and larger step sizes led to unfolding events outside the cluster, suggesting additional unfolding in the remaining GAIN B subdomain of GPR56-T383G (Figure S1B–D). This further unfolding was prevented in wild-type GPR56 due to NTF/CTF dissociation.

MECHANICAL RESPONSES OF BAI3 GAIN DOMAIN DURING FORCE LOADING

As the GAIN domain of BAI3 is not cleavable, our examination of the BAI3 GAIN domain focused on force-dependent conformational changes. Since the GAIN domain is not cleaved, it can be repeatedly unfolded and refolded. Figure 4A displays representative force–bead height curves obtained from a BAI3 construct subjected to multiple consecutive force-loading processes. Following each loading, the force was reduced to 1 pN for 30 s to allow the domains to refold.

The curves show complex multiple stages of unfolding signals during each force-loading process. When the force exceeds 30 pN, the curves overlap, indicating complete unfolding of all the structural elements within the GAIN. Based on the force-dependent step sizes and assuming a typical bending persistence of 0.8 nm for low-force response of polypeptide polymers,[48,52] it is estimated that more than 280 amino acids of polypeptide were released after unfolding (Supplementary Text S2). This suggests that the majority of GAIN and HormR domains of BAI3, comprising around 366 amino acid residues, unfold at forces above 30 pN.

At forces between 5 and 10 pN, there are two unfolding steps, which are sometimes combined into a single step of unfolding. The step sizes of the first unfolding steps ranging from 10–30 nm are similar to the partial unfolding signals observed for GPR56 and LPHN1 preceding the NTF/CTF dissociation (circled orange data cluster in Figure 4B, obtained from over 10 tethers).

DIRECT VISUALIZATION OF GAIN DOMAIN CLEAVAGE DURING CELL MIGRATION

The NTFs of aGPCRs contain domains that are capable of associating with the ECM or membrane receptors on other cells. This association is necessary to establish the mechanical stretching of aGPCRs. We tested whether force transmitted on such a linkage would result in NTF/CTF dissociation during cell migration, using a cell-based assay that allows for direct visualization of the dissociation of NTF and CTF of GPR56. An artificial covalent ligand was used to form a stable linkage between the NTF and ECM.

We created two GPR56 constructs: Spy-GPR56-WT-GFP and Spy-GPR56-T383A-GFP. We inserted a SpyTag between the signal peptide and the pentraxin and laminin/neurexin/sex hormone-binding globulin-like (PLL) domain and added a GFP tag after the 7TM domains in both constructs (Figure 5A). The Spy-GPR56-T383A-GFP contains a mutated non-cleavable GAIN domain,[53] while Spy-GPR56-WT-GFP's GAIN domain was cleavable. We confirmed the cleavage ability of Spy-GPR56-WT-GFP and the inability of Spy-GPR56-T383A-GFP to undergo GAIN domain cleavage through independent Western blot analysis (Figure 5B).

https://doi.org/10.1021/acs.nanolett.3c01163
Nano Lett. XXXX, XXX, XXX–XXX

We transfected human foreskin fibroblast (HFF) cells, which do not express endogenous GPR56, with either Spy-GPR56-WT-GFP or Spy-GPR56-T383A-GFP. The cells were then seeded onto fibronectin mixed with SpyCatcher, referred to as the FN+Spy surface, to provide an integrin-based substrate for cell migration. SpyCatcher acted as an artificial ligand that could covalently associate with the SpyTag on the NTFs of Spy-GPR56-WT-GFP and Spy-GPR56-T383A-GFP. The resulting covalent bond between SpyCatcher and SpyTag allowed the cleaved NTFs to be retained on the surface for later immunostaining analysis.

Our observations indicate that Spy-GPR56-WT-GFP was clearly cleaved on the FN+Spy surface, as shown by the miscolocalization of the receptor's N-terminal and C-terminal regions. In contrast, cells expressing the noncleavable Spy-GPR56-T383A-GFP exhibited well-co-localized N-terminal and C-terminal regions on the FN+Spy surfaces (Figure 5C). Pearson's correlation coefficients supported these findings (Figure 5D). These results indicate that NTF/CTF dissociation occurred during the cell migration.

In summary, we examined the mechanical responses of two autocleavable aGPCRs (GPR56 and LPHN1), a noncleavable aGPCR (BAI3), and a cleavage-deficient GPR56-T383G mutant at a single-molecule level using magnetic tweezers. We discovered that all three GAIN domains are sensitive to forces ranging from a few to approximately 20 pN at a physiologically relevant force-loading rate of 1 pN/s. NTF/CTF dissociation for GPR56 and LPHN1 occurs at forces between 10 and 20 pN, following the partial unfolding of the GAINs. Using SpyCatcher as an artificial ligand, we demonstrated dissociation of NTF from CTF in a cell migration assay. Overall, these findings show that the GAIN domains' structural integrity is precisely regulated by pN forces and forces produced during cell migration.

Understanding the forces that unfold the GAIN domain and dissociate the NTF/CTF complex during force loading at a rate of 1 pN/s is crucial in physiological contexts, as this loading rate is highly physiologically relevant (Supplementary Text S3). It is plausible that GAIN domain unfolding could reveal the Stachel sequence and promote NTF/CTF subunit dissociation,[26] aligning with our observations in the cell migration assay using a SpyCatcher−SpyTag linkage.

The observation of similar partial unfolding signals in the GAIN domains preceding the dissociation of the Stachel sequence from the GAIN B subdomains of GPR56 and LPHN1 is intriguing. The differing sizes of their GAIN A subdomains lead to distinct stretching geometries.[54] While the different stretching geometries are expected to have a significant impact on the mechanical stability of protein domains,[55,56] it was not observed in the partial unfolding signals of the GAIN domains in this study. This suggests a potential transition pathway starting from the disruption of the interaction between the GAIN A and GAIN B subdomains. As a result, the GAIN B subdomain experiences consistent force geometry (Figure S2), leading to similar partial unfolding signals prior to Stachel sequence dissociation from the GAIN B subdomain.

Our data suggest that the unfolding of the GAIN B subdomain may facilitate the dissociation of the cleaved Stachel sequence. The structural features of the GAIN B subdomain, as seen in LPHN1 and BAI3,[11] reveal that the Stachel sequence is inserted into a deep pocket within the GAIN B subdomain, stabilized with hydrophobic interactions and multiple hydrogen bonds within the pocket (Figure S3). Additionally, the Stachel sequence adopts a pre-extended conformation under a shear-force geometry, which was expected to result in mechanical stabilization (catch-bond kinetics).[56,57] Therefore, direct dissociation of the cleaved Stachel sequence from the pocket without partial unfolding of the GAIN B subdomain seems challenging. Hence, we propose that partial unfolding of the GAIN B subdomain promotes dissociation of the Stachel sequence by disrupting interactions with surrounding residues in the GAIN B subdomain.

Based on current knowledge, the exposure of the cryptic Stachel sequence within the GAIN B subdomain appears to be crucial for activating aGPCRs.[12,13] Intuitively, mechanical dissociation of the Stachel sequence from the GAIN B subdomain could fully expose the Stachel sequence, thereby activating the aGPCRs.[58] A recent study from one of our laboratories suggests that NTF/CTF dissociation indeed occurs *in vivo* and is necessary for the noncell-autonomous effects of aGPCRs.[26] However, the presence of various mechanosensitive aGPCRs that possess a nonself-cleaved GAIN B subdomain raises questions about the necessity of GAIN B subdomain dissociation for the mechanical activation of aGPCRs. It is possible that a partially unfolded GAIN B subdomain could also expose enough of the Stachel sequence to achieve activation as suggested before by us[10,17,27] and others.[24,28]

Our study shows that a 1 pN/s loading rate results in conserved GAIN domain partial unfolding over pN forces for all three aGPCRs tested by comparing mechanical properties across subfamilies B, G, and L. Additionally, GPR56 and LPHN1 display extensive GAIN domain partial unfolding before NTF/CTF dissociation. In addition to the investigations of GPR56, LPHN1, and BAI3 presented in this work, the mechanical response of another aGPCR, LPHN3, has been studied by Zhong et al.[59] They also observed a similar partial unfolding event that precedes the NTF/CTF dissociation at similar forces. These findings indicate that GAIN domain mechanosensitivity during physiological stretching is likely a conserved property among aGPCRs. The observed partial GAIN domain unfolding preceding Stachel dissociation suggests an intermediate state where the autocleaved Stachel sequence becomes unstable. Although our data indicate that the partial unfolding signal mainly involves the GAIN B subdomain, it is likely that a disruption between GAIN A and GAIN B subdomains also occurs.

While our study offers insights into the force-dependent unfolding of the GAIN domain and NTF/CTF dissociation, there are several limitations needed to be addressed in future studies to further understand the physiological relevance of these findings.

Our single-molecule study is limited to *in vitro* experiments, while *in vivo* aGPCRs could experience a more complex mechanical force environment, such as a wider range of loading rate or limited force duration. Additionally, our single-molecule study was conducted using purified GAIN domains. While this aligns with a primary focus to investigate the mechanical responses of the extracellular GAIN domains, we cannot disregard the possibility that the nearby membrane might create a distinct environment through nonspecific binding with the GAIN domains, potentially affecting their mechanical responses.

Furthermore, our cell spreading assay used an artificial SpyCatcher ligand that forms a covalent bond with the NTF of

https://doi.org/10.1021/acs.nanolett.3c01163
Nano Lett. XXXX, XXX, XXX−XXX

GPR56, while physiological ligand−NTF interfaces are noncovalent and have limited lifetimes. The force-dependent lifetime of these interfaces remains undetermined, and understanding it is crucial for interpreting the aGPCR-mediated mechanosensing and mechanotransduction. Although our observations do not explain how GAIN unfolding and NTF/CTF dissociation lead to mechanical activation of aGPCRs, previous studies suggest complementary approaches[60,61] for future investigation. Comprehensive studies are required to fully understand the role of mechanical activation in aGPCR signaling, which is the focus of our ongoing research.

In conclusion, this study offers valuable insights into the mechanical activation of aGPCRs.[9,62] The findings indicate that GAIN domain stability and NTF/CTF dissociation are responsive to physiological tensile forces. Further research is needed to establish the physiological relevance of and comprehend the role of mechanical activation in aGPCR signaling. This knowledge may aid in developing targeted drugs and understanding the role of aGPCRs in diverse physiological processes.

MAGNETIC TWEEZER-BASED SINGLE-MOLECULE FORCE APPROACH

The single-molecule manipulation experiments were carried out on a custom-built magnetic-tweezers setup[63] that record bead images at a 200 Hz sampling rate. The method we used to calibrate forces has a 10% uncertainty due to the heterogeneous manufactured bead sizes.[49,63] The detailed protocols of channel and sample preparation, magnetic tweezer setup, and force calibration were published in our previous studies[49] and are briefly shown in Supplementary Text S1.

More details on protein expression and purification, cell culture and transfection, immunofluorescence staining, Western blot, and data analysis can be found in Supplementary Text S4.

ASSOCIATED CONTENT

Supporting Information

The Supporting Information is available free of charge at https://pubs.acs.org/doi/10.1021/acs.nanolett.3c01163.

Force-induced unfolding of the GAIN domains of GRP56 and GPR56-T383G (Figure S1); force geometry of GPR56, LPHN1, and BAI3 (Figure S2); structural insights into the interactions between the Stachel sequence and surrounding residues (Figure S3); additional materials and methods of channel, bead, and sample preparation and force calibration and force extension curves (Supplementary Text S1); evidence of partial unfolding of GAIN B subdomain preceding NTF/CTF dissociation (Supplementary Text S2); additional discussion of physiologically relevance of force loading rate used in the study (Supplementary Text S3); and additional materials and methods of protein expression and purification, cell culture and transfection, immunofluorescence staining, Western blot, and data analysis (Supplementary Text S4) (PDF)

AUTHOR INFORMATION

Corresponding Authors

Gaojie Song − *School of Life Sciences, East China Normal University, Shanghai 200241, China*; Email: gjsong@bio.ecnu.edu.cn

Jie Yan − *Department of Physics, National University of Singapore, Singapore 117551, Singapore; Mechanobiology Institute, National University of Singapore, Singapore 117411, Singapore; Centre for Bioimaging Sciences, National University of Singapore, Singapore 117557, Singapore; Joint School of National University of Singapore and Tianjin University, International Campus of Tianjin University, Binhai New City, Fuzhou 350207, China*; orcid.org/0000-0002-8555-7291; Email: phyyj@nus.edu.sg

Authors

Chaoyu Fu − *Department of Physics, National University of Singapore, Singapore 117551, Singapore; Mechanobiology Institute, National University of Singapore, Singapore 117411, Singapore*

Wenmao Huang − *Department of Physics, National University of Singapore, Singapore 117551, Singapore; Mechanobiology Institute, National University of Singapore, Singapore 117411, Singapore*

Qingnan Tang − *Department of Physics, National University of Singapore, Singapore 117551, Singapore*

Minghui Niu − *School of Life Sciences, East China Normal University, Shanghai 200241, China*

Shiwen Guo − *Mechanobiology Institute, National University of Singapore, Singapore 117411, Singapore*

Tobias Langenhan − *Rudolf Schönheimer Institute of Biochemistry, Division of General Biochemistry, Medical Faculty, Leipzig University, Leipzig 04103, Germany*

Complete contact information is available at: https://pubs.acs.org/10.1021/acs.nanolett.3c01163

Author Contributions

#C.F., W.H., and Q.T. contributed equally to this work. C.F., W.H., Q.T., and S.G. performed the experiments; G.S. and J.Y. designed the single-molecule studies. M.N. expressed and purified the protein constructs. C.F., T.L., and J.Y. designed the cell migration assay. G.S. and J.Y. cosupervised the single-molecule studies.

Notes

The authors declare no competing financial interest.

ACKNOWLEDGMENTS

J.Y. acknowledges funding by the Singapore Ministry of Education Academic Research Funds Tier 2 (MOE-T2EP50220-0015), the Singapore Ministry of Education Academic Research Fund Tier 3 (MOE Grant No. MOET32021-0003), and the Ministry of Education under the Research Centres of Excellence programme. T.L. acknowledges funding by the Deutsche Forschungsgemeinschaft through SFB1423, project number 421152132, subproject B06. G.S. acknowledges funding by the National Nature Science Foundation of China Grant 31770898.

REFERENCES

(1) Hilger, D.; Masureel, M.; Kobilka, B. K. Structure and dynamics of GPCR signaling complexes. *Nature structural & molecular biology* **2018**, *25*, 4−12.

(2) Purcell, R. H.; Hall, R. A. Adhesion G Protein−Coupled Receptors as Drug Targets. *Annual review of pharmacology and toxicology* **2018**, *58*, 429−449.
(3) Civelli, O.; Reinscheid, R. K.; Zhang, Y.; Wang, Z.; Fredriksson, R.; Schiöth, H. B. G protein−coupled receptor deorphanizations. *Annual review of pharmacology and toxicology* **2013**, *53*, 127−146.
(4) Lagerström, M. C.; Schiöth, H. B. Structural diversity of G protein-coupled receptors and significance for drug discovery. *Nat. Rev. Drug Discovery* **2008**, *7*, 339−357.
(5) Schiöth, H. B.; Fredriksson, R. The GRAFS classification system of G-protein coupled receptors in comparative perspective. *General and comparative endocrinology* **2005**, *142*, 94−101.
(6) Araç, D., Sträter, N., Seiradake, E. In *Adhesion G Protein-coupled Receptors: Molecular, Physiological and Pharmacological Principles in Health and Disease*; Langenhan, T., Schöneberg, T., Eds.; Handbook of Experimental Pharmacology; Springer, 2016; Vol. *234*; pp 67−82.
(7) McKnight, A. J.; Gordon, S. The EGF-TM7 family: unusual structures at the leukocyte surface. *Journal of leukocyte biology* **1998**, *63*, 271−280.
(8) Hamann, J.; Aust, G.; Araç, D.; Engel, F. B.; Formstone, C.; Fredriksson, R.; Hall, R. A.; Harty, B. L.; Kirchhoff, C.; Knapp, B.; et al. International union of basic and clinical pharmacology. xciv. adhesion g protein-coupled receptors. *Pharmacol. Rev.* **2015**, *67*, 338−367.
(9) Vizurraga, A.; Adhikari, R.; Yeung, J.; Yu, M.; Tall, G. G. Mechanisms of adhesion G protein-coupled receptor activation. *J. Biol. Chem.* **2020**, *295*, 14065−14083.
(10) Prömel, S.; Frickenhaus, M.; Hughes, S.; Mestek, L.; Staunton, D.; Woollard, A.; Vakonakis, I.; Schöneberg, T.; Schnabel, R.; Russ, A. P.; et al. The GPS motif is a molecular switch for bimodal activities of adhesion class G protein-coupled receptors. *Cell reports* **2012**, *2*, 321−331.
(11) Araç, D.; Boucard, A. A.; Bolliger, M. F.; Nguyen, J.; Soltis, S. M.; Südhof, T. C.; Brunger, A. T. A novel evolutionarily conserved domain of cell-adhesion GPCRs mediates autoproteolysis. *EMBO journal* **2012**, *31*, 1364−1378.
(12) Stoveken, H. M.; Hajduczok, A. G.; Xu, L.; Tall, G. G. Adhesion G protein-coupled receptors are activated by exposure of a cryptic tethered agonist. *Proc. Natl. Acad. Sci. U. S. A.* **2015**, *112*, 6194−6199.
(13) Liebscher, I.; Schön, J.; Petersen, S. C.; Fischer, L.; Auerbach, N.; Demberg, L. M.; Mogha, A.; Cöster, M.; Simon, K.-U.; Rothemund, S.; et al. A tethered agonist within the ectodomain activates the adhesion G protein-coupled receptors GPR126 and GPR133. *Cell reports* **2014**, *9*, 2018−2026.
(14) Gray, J. X.; Haino, M.; Roth, M. J.; Maguire, J. E.; Jensen, P. N.; Yarme, A.; Stetler-Stevenson, M.-A.; Siebenlist, U.; Kelly, K. CD97 is a processed, seven-transmembrane, heterodimeric receptor associated with inflammation. *J. Immunol.* **1996**, *157*, 5438−5447.
(15) Krasnoperov, V. G.; Bittner, M. A.; Beavis, R.; Kuang, Y.; Salnikow, K. V.; Chepurny, O. G.; Little, A. R.; Plotnikov, A. N.; Wu, D.; Holz, R. W.; et al. α-Latrotoxin stimulates exocytosis by the interaction with a neuronal G-protein-coupled receptor. *Neuron* **1997**, *18*, 925−937.
(16) Lin, H.-H.; Chang, G.-W.; Davies, J. Q.; Stacey, M.; Harris, J.; Gordon, S. Autocatalytic cleavage of the EMR2 receptor occurs at a conserved G protein-coupled receptor proteolytic site motif. *J. Biol. Chem.* **2004**, *279*, 31823−31832.
(17) Beliu, G.; Altrichter, S.; Guixà-González, R.; Hemberger, M.; Brauer, I.; Dahse, A.-K.; Scholz, N.; Wieduwild, R.; Kuhlemann, A.; Batebi, H.; et al. Tethered agonist exposure in intact adhesion/class B2 GPCRs through intrinsic structural flexibility of the GAIN domain. *Molecular cell* **2021**, *81*, 905−921.
(18) Langenhan, T. Adhesion G protein-coupled receptors−Candidate metabotropic mechanosensors and novel drug targets. *Basic Clin Pharmacol Toxicol* **2020**, *126*, 5−16.
(19) Langenhan, T.; Piao, X.; Monk, K. R. Adhesion G protein-coupled receptors in nervous system development and disease. *Nat. Rev. Neurosci.* **2016**, *17*, 550−561.
(20) Scholz, N. Cancer cell mechanics: adhesion G protein-coupled receptors in action? *Frontiers in oncology* **2018**, *8*, 59.
(21) Kan, Z.; Jaiswal, B. S.; Stinson, J.; Janakiraman, V.; Bhatt, D.; Stern, H. M.; Yue, P.; Haverty, P. M.; Bourgon, R.; Zheng, J.; et al. Diverse somatic mutation patterns and pathway alterations in human cancers. *Nature* **2010**, *466*, 869−873.
(22) Folts, C. J.; Giera, S.; Li, T.; Piao, X. Adhesion G protein-coupled receptors as drug targets for neurological diseases. *Trends in pharmacological sciences* **2019**, *40*, 278−293.
(23) Lin, H.-H.; Hsiao, C.-C.; Pabst, C.; Hébert, J.; Schöneberg, T.; Hamann, J. Adhesion GPCRs in regulating immune responses and inflammation. *Advances in immunology* **2017**, *136*, 163−201.
(24) Liu, D.; Duan, L.; Rodda, L. B.; Lu, E.; Xu, Y.; An, J.; Qiu, L.; Liu, F.; Looney, M. R.; Yang, Z.; et al. CD97 promotes spleen dendritic cell homeostasis through the mechanosensing of red blood cells. *Science* **2022**, *375*, eabi5965.
(25) Yeung, J.; Adili, R.; Stringham, E. N.; Luo, R.; Vizurraga, A.; Rosselli-Murai, L. K.; Stoveken, H. M.; Yu, M.; Piao, X.; Holinstat, M.; et al. GPR56/ADGRG1 is a platelet collagen-responsive GPCR and hemostatic sensor of shear force. *Proc. Natl. Acad. Sci. U. S. A.* **2020**, *117*, 28275−28286.
(26) Scholz, N.; Dahse, A.-K.; Kemkemer, M.; Bormann, A.; Auger, G. M.; Vieira Contreras, F.; Ernst, L. F.; Staake, H.; Körner, M. B.; Buhlan, M.; et al. Molecular sensing of mechano-and ligand-dependent adhesion GPCR dissociation. *Nature* **2023**, *615*, 945−953.
(27) Scholz, N.; Guan, C.; Nieberler, M.; Grotemeyer, A.; Maiellaro, I.; Gao, S.; Beck, S.; Pawlak, M.; Sauer, M.; Asan, E.; et al. Mechano-dependent signaling by Latrophilin/CIRL quenches cAMP in proprioceptive neurons. *Elife* **2017**, *6*, e28360.
(28) Sando, R.; Jiang, X.; Südhof, T. C. Latrophilin GPCRs direct synapse specificity by coincident binding of FLRTs and teneurins. *Science* **2019**, *363*, eaav7969.
(29) Barros-Álvarez, X.; Nwokonko, R. M.; Vizurraga, A.; Matzov, D.; He, F.; Papasergi-Scott, M. M.; Robertson, M. J.; Panova, O.; Yardeni, E. H.; Seven, A. B.; et al. The tethered peptide activation mechanism of adhesion GPCRs. *Nature* **2022**, *604*, 757−762.
(30) Xiao, P.; Guo, S.; Wen, X.; He, Q.-T.; Lin, H.; Huang, S.-M.; Gou, L.; Zhang, C.; Yang, Z.; Zhong, Y.-N.; et al. Tethered peptide activation mechanism of the adhesion GPCRs ADGRG2 and ADGRG4. *Nature* **2022**, *604*, 771−778.
(31) Qu, X.; Qiu, N.; Wang, M.; Zhang, B.; Du, J.; Zhong, Z.; Xu, W.; Chu, X.; Ma, L.; Yi, C.; et al. Structural basis of tethered agonism of the adhesion GPCRs ADGRD1 and ADGRF1. *Nature* **2022**, *604*, 779−785.
(32) Ping, Y.-Q.; Xiao, P.; Yang, F.; Zhao, R.-J.; Guo, S.-C.; Yan, X.; Wu, X.; Zhang, C.; Lu, Y.; Zhao, F.; et al. Structural basis for the tethered peptide activation of adhesion GPCRs. *Nature* **2022**, *604*, 763−770.
(33) Lin, H.; Xiao, P.; Bu, R.-Q.; Guo, S.; Yang, Z.; Yuan, D.; Zhu, Z.-L.; Zhang, C.-X.; He, Q.-T.; Zhang, C.; et al. Structures of the ADGRG2-Gs complex in apo and ligand-bound forms. *Nat. Chem. Biol.* **2022**, *18*, 1196−1203.
(34) Qian, Y.; Ma, Z.; Liu, C.; Li, X.; Zhu, X.; Wang, N.; Xu, Z.; Xia, R.; Liang, J.; Duan, Y.; et al. Structural insights into adhesion GPCR ADGRL3 activation and Gq, Gs, Gi, and G12 coupling. *Mol. Cell* **2022**, *82*, 4340−4352.
(35) Zhu, X.; Qian, Y.; Li, X.; Xu, Z.; Xia, R.; Wang, N.; Liang, J.; Yin, H.; Zhang, A.; Guo, C.; et al. Structural basis of adhesion GPCR GPR110 activation by stalk peptide and G-proteins coupling. *Nat. Commun.* **2022**, *13*, 5513.
(36) Petersen, S. C.; Luo, R.; Liebscher, I.; Giera, S.; Jeong, S.-J.; Mogha, A.; Ghidinelli, M.; Feltri, M. L.; Schöneberg, T.; Piao, X.; et al. The adhesion GPCR GPR126 has distinct, domain-dependent functions in Schwann cell development mediated by interaction with laminin-211. *Neuron* **2015**, *85*, 755−769.
(37) Scholz, N.; Gehring, J.; Guan, C.; Ljaschenko, D.; Fischer, R.; Lakshmanan, V.; Kittel, R. J.; Langenhan, T. The adhesion GPCR latrophilin/CIRL shapes mechanosensation. *Cell reports* **2015**, *11*, 866−874.

https://doi.org/10.1021/acs.nanolett.3c01163
Nano Lett. XXXX, XXX, XXX−XXX

(38) Boyden, S. E.; Desai, A.; Cruse, G.; Young, M. L.; Bolan, H. C.; Scott, L. M.; Eisch, A. R.; Long, R. D.; Lee, C.-C. R.; Satorius, C. L.; et al. Vibratory urticaria associated with a missense variant in ADGRE2. *New England Journal of Medicine* **2016**, *374*, 656−663.
(39) Karpus, O. N.; Veninga, H.; Hoek, R. M.; Flierman, D.; van Buul, J. D.; Vandenakker, C. C.; vanBavel, E.; Medof, M. E.; van Lier, R. A.; Reedquist, K. A.; et al. Shear stress-dependent downregulation of the adhesion-G protein-coupled receptor CD97 on circulating leukocytes upon contact with its ligand CD55. *J. Immunol.* **2013**, *190*, 3740−3748.
(40) White, J. P.; Wrann, C. D.; Rao, R. R.; Nair, S. K.; Jedrychowski, M. P.; You, J.-S.; Martínez-Redondo, V.; Gygi, S. P.; Ruas, J. L.; Hornberger, T. A.; et al. G protein-coupled receptor 56 regulates mechanical overload-induced muscle hypertrophy. *Proc. Natl. Acad. Sci. U. S. A.* **2014**, *111*, 15756−15761.
(41) Wilde, C.; Fischer, L.; Lede, V.; Kirchberger, J.; Rothemund, S.; Schöneberg, T.; Liebscher, I. The constitutive activity of the adhesion GPCR GPR114/ADGRG5 is mediated by its tethered agonist. *FASEB J.* **2016**, *30*, 666−673.
(42) Liebscher, I.; Schöneberg, T. In *Adhesion G Protein-coupled Receptors: Molecular, Physiological and Pharmacological Principles in Health and Disease*; Langenhan, T., Schöneberg, T., Eds.; Handbook of Experimental Pharmacology; 2016; Vol. *234*; Springer, 2016; pp 111−125.
(43) Kishore, A.; Hall, R. A. In *Adhesion G Protein-coupled Receptors: Molecular, Physiological and Pharmacological Principles in Health and Disease*; Langenhan, T., Schöneberg, T., Eds.; Handbook of Experimental Pharmacology; Springer, 2016; Vol. *234*; pp 127−146.
(44) Nieberler, M.; Kittel, R. J.; Petrenko, A. G.; Lin, H.-H.; Langenhan, T. In *Adhesion G Protein-coupled Receptors: Molecular, Physiological and Pharmacological Principles in Health and Disease*; Langenhan, T., Schöneberg, T., Eds.; Handbook of Experimental Pharmacology; Springer, 2016; Vol. *234*; pp 83−109.
(45) Sigoillot, S. M.; Monk, K. R.; Piao, X.; Selimi, F.; Harty, B. L. In *Adhesion G Protein-coupled Receptors: Molecular, Physiological and Pharmacological Principles in Health and Disease*; Langenhan, T., Schöneberg, T., Eds.; Handbook of Experimental Pharmacology; Springer, 2016; Vol. *234*; pp 275−298.
(46) Roca-Cusachs, P.; Conte, V.; Trepat, X. Quantifying forces in cell biology. *Nature cell biology* **2017**, *19*, 742−751.
(47) Huse, M. Mechanical forces in the immune system. *Nature Reviews Immunology* **2017**, *17*, 679−690.
(48) Chen, H.; Fu, H.; Zhu, X.; Cong, P.; Nakamura, F.; Yan, J. Improved high-force magnetic tweezers for stretching and refolding of proteins and short DNA. *Biophysical journal* **2011**, *100*, 517−523.
(49) Zhao, X.; Zeng, X.; Lu, C.; Yan, J. Studying the mechanical responses of proteins using magnetic tweezers. *Nanotechnology* **2017**, *28*, 414002.
(50) Salzman, G. S.; Ackerman, S. D.; Ding, C.; Koide, A.; Leon, K.; Luo, R.; Stoveken, H. M.; Fernandez, C. G.; Tall, G. G.; Piao, X.; et al. Structural basis for regulation of GPR56/ADGRG1 by its alternatively spliced extracellular domains. *Neuron* **2016**, *91*, 1292−1304.
(51) Zakeri, B.; Fierer, J. O.; Celik, E.; Chittock, E. C.; Schwarz-Linek, U.; Moy, V. T.; Howarth, M. Peptide tag forming a rapid covalent bond to a protein, through engineering a bacterial adhesin. *Proc. Natl. Acad. Sci. U. S. A.* **2012**, *109*, E690−E697.
(52) Yao, M.; Goult, B. T.; Klapholz, B.; Hu, X.; Toseland, C. P.; Guo, Y.; Cong, P.; Sheetz, M. P.; Yan, J. The mechanical response of talin. *Nat. Commun.* **2016**, *7*, 11966.
(53) Kishore, A.; Purcell, R. H.; Nassiri-Toosi, Z.; Hall, R. A. Stalk-dependent and stalk-independent signaling by the adhesion G protein-coupled receptors GPR56 (ADGRG1) and BAI1 (ADGRB1). *J. Biol. Chem.* **2016**, *291*, 3385−3394.
(54) Wang, F.; Wang, Y.; Qiu, W.; Zhang, Q.; Yang, H.; Song, G. Crystal Structure of the Extracellular Domains of GPR110. *J. Mol. Biol.* **2023**, *435*, 167979.
(55) Gao, Y.; Sirinakis, G.; Zhang, Y. Highly anisotropic stability and folding kinetics of a single coiled coil protein under mechanical tension. *J. Am. Chem. Soc.* **2011**, *133*, 12749−12757.
(56) Guo, S.; Tang, Q.; Yao, M.; You, H.; Le, S.; Chen, H.; Yan, J. Structural-elastic determination of the force-dependent transition rate of biomolecules. *Chemical science* **2018**, *9*, 5871−5882.
(57) Huang, W.; Le, S.; Sun, Y.; Lin, D. J.; Yao, M.; Shi, Y.; Yan, J. Mechanical stabilization of a bacterial adhesion complex. *J. Am. Chem. Soc.* **2022**, *144*, 16808−16818.
(58) Frenster, J. D.; Stephan, G.; Ravn-Boess, N.; Bready, D.; Wilcox, J.; Kieslich, B.; Wilde, C.; Sträter, N.; Wiggin, G. R.; Liebscher, I.; et al. Functional impact of intramolecular cleavage and dissociation of adhesion G protein-coupled receptor GPR133 (ADGRD1) on canonical signaling. *J. Biol. Chem.* **2021**, *296*, 100798.
(59) Zhong, B. L.; Lee, C. E.; Vachharajani, V. T.; Bauer, M. s.; Sudhof, T. C.; Dunn, A. R. Piconewton forces mediate GAIN domain dissociation of the latrophilin−3 adhesion GPCR. *Nano Lett.* **2023**.
(60) Stephan, G.; Frenster, J. D.; Liebscher, I.; Placantonakis, D. G. Activation of the adhesion G protein-coupled receptor GPR133 by antibodies targeting its N-terminus. *J. Biol. Chem.* **2022**, *298*, 101949.
(61) Mitgau, J.; Franke, J.; Schinner, C.; Stephan, G.; Berndt, S.; Placantonakis, D. G.; Kalwa, H.; Spindler, V.; Wilde, C.; Liebscher, I. The N Terminus of Adhesion G Protein-Coupled Receptor GPR126/ADGRG6 as Allosteric Force Integrator. *Frontiers in Cell and Developmental Biology* **2022**, *10*, 873278.
(62) Scholz, N.; Monk, K. R.; Kittel, R. J.; Langenhan, T. In *Adhesion G Protein-coupled Receptors: Molecular, Physiological and Pharmacological Principles in Health and Disease*; Langenhan, T., Schöneberg, T., Eds.; Handbook of Experimental Pharmacology; Springer, 2016; Vol. *234*; pp 221−247.
(63) Chen, H.; Nakamura, F.; Fu, H.; Cong, P.; Sheetz, M. P.; Yan, J. Unfolding and Refolding Dynamics of Filamin a Protein under Constant Forces. *Biophys. J.* **2010**, *98*, 753a.

https://doi.org/10.1021/acs.nanolett.3c01163
Nano Lett. XXXX, XXX, XXX−XXX